

The tensile strength of dust aggregates consisting of small elastic grains: constraints on the size of condensates in protoplanetary discs

Hiroshi Kimura,^{*} Koji Wada, Fumi Yoshida, Peng K. Hong, Hiroki Senshu, Tomoko Arai, Takayuki Hirai, Masanori Kobayashi, Ko Ishibashi and Manabu Yamada
Planetary Exploration Research Center (PERC), Chiba Institute of Technology, Tsudanuma 2-17-1, Narashino, Chiba 275-0016, Japan

Accepted 2020 June 4. Received 2020 June 3; in original form 2020 May 2

ABSTRACT

A consensus view on the formation of planetesimals is now exposed to a threat, since recent numerical studies on the mechanical properties of dust aggregates tend to dispute the conceptual picture that submicrometer-sized grains conglomerate into planetesimals in protoplanetary discs. With the advent of precise laboratory experiments and extensive computer simulations on the interaction between elastic spheres comprising dust aggregates, we revisit a model for the tensile strength of dust aggregates consisting of small elastic grains. In the framework of contact mechanics and fracture mechanics, we examine outcomes of computer simulations and laboratory experiments on the tensile strength of dust aggregates. We provide a novel analytical formula that explicitly incorporates the volume effect on the tensile strength, namely, the dependence of tensile strength on the volume of dust aggregates. We find that our model for the tensile strength of dust aggregates well reproduces results of computer simulations and laboratory experiments, if appropriate values are adopted for the elastic parameters used in the model. Moreover, the model with dust aggregates of submicrometer-sized grains is in good harmony with the tensile strength of cometary dust and meteoroids derived from astronomical observations. Therefore, we reaffirm the commonly believed idea that the formation of planetesimals begins with conglomeration of submicrometer-sized grains condensed in protoplanetary discs.

Key words: comets: general – meteorites, meteors, meteoroids – protoplanetary discs – zodiacal dust – planets and satellites: fundamental parameters – (ISM:) dust, extinction

1 INTRODUCTION

The condensation of gas into solid minute grains and the subsequent aggregation of dust grains into planetesimals are believed to be the sequence of events in protoplanetary discs that leads to the formation of planets. There is a common belief that the constituent grains of dust aggregates in protoplanetary discs have a radius of submicrometers, owing to so much evidence of submicrometer-sized grains conglomerated into planetesimals: A nucleation theory implies that the formation of grains in a protoplanetary disc with solar composition is in accordance with the submicrometer size of condensates in the solar nebula (Yamamoto & Hasegawa 1977); The spectral and angular dependences of brightness and polarization of cometary comae measured in the visible wavelength range cannot be simultaneously reproduced unless aggregates are composed of submicrometer-sized grains with a radius of $r_0 = 0.1 \mu\text{m}$ (Kimura, Kolokolova & Mann 2003, 2006); Infrared spectral features of forsterite observed in thermal emission from cometary comae are inevitably attributed to porous dust aggregates of constituent grains smaller than micrometers in radius (Okamoto, Mukai & Kozasa 1994; Kolokolova et al. 2007); The stratospheric

^{*} E-mail: hiroshi_kimura@perc.it-chiba.ac.jp

collection of interplanetary dust particles (IDPs) by NASA identifies the chondritic porous (CP) subset of IDPs to be of cometary origin and to be aggregates of submicron grains (e.g. [Brownlee 1985](#)); AFM topographic images of dust aggregates collected in the coma of comet 67P/Churyumov-Gerasimenko (hereafter, 67P/C-G) by MIDAS onboard Rosetta demonstrate without doubt that the constituent grains of dust aggregates in 67P/C-G are submicrometer in radius ([Bentley et al. 2016](#); [Mannel et al. 2016](#)); The mechanical and electric properties of dust aggregates in the coma of comet 67P/C-G measured by COSIMA/Rosetta are also in harmony with the picture that submicrometer-sized constituent grains with $r_0 = 0.1 \mu\text{m}$ make up the aggregates ([Kimura et al. 2020](#)); [Weidenschilling \(1984, 1997\)](#) assumed a slightly larger constituent grains with $r_0 = 0.5 \mu\text{m}$ to model the growth of dust aggregates in protoplanetary discs without justification of the grain size ([Weidenschilling, Donn & Meakin 1989](#)). Accordingly, there was no single convincing report against the submicrometer-sized grains in dust aggregates that form planetesimals in protoplanetary discs, as far as we know.

What came as a great surprise is that recent studies on the mechanical properties of dust aggregates in protoplanetary discs shed doubt on the consensus about the size of constituent grains (hereafter, monomers) in dust aggregates. [Arakawa & Nakamoto \(2016\)](#) claimed the formation of rocky planetesimals through intense cohesion of nanometer-sized silicate monomers that were produced by evaporation of presolar submicrometer-sized silicate grains in protoplanetary discs and subsequent condensation of the vapor. However, they seem to have overlooked one important evidence that cohesion of submicrometer-sized silicate grains has been one order of magnitude underestimated in former times ([Kimura et al. 2015](#)). [Okamoto & Nakamura \(2017\)](#) conducted impact crating experiments on highly porous targets and applied their new empirical scaling law to comet 9P/Tempel 1. According to their estimates of the tensile strength, the monomers of dust aggregates in 9P/Tempel 1 have large radii of $r_0 = 45\text{--}1050 \mu\text{m}$, but it is odd that the monomers comprising dust aggregates are larger than the aggregates with a typical radius of $R \approx 40 \mu\text{m}$ in 9P/Tempel 1 (cf. [Kobayashi, Kimura & Yamamoto 2013](#)). On the basis of their numerical simulation on the tensile strength of porous dust aggregates, [Tatsuuma, Kataoka & Tanaka \(2019\)](#) proposed a radius of $r_0 = 3.3\text{--}220 \mu\text{m}$ for the monomers of dust aggregates in 67P/C-G, instead of $r_0 \sim 0.1 \mu\text{m}$ as commonly believed. While they provide an empirical formula that reproduces their numerical results, it turned out that if $r_0 = 0.1 \mu\text{m}$, their formula significantly overestimates the tensile strength estimated for overhangs on the surface of comet 67P/C-G. In addition, their empirical formula predicts a value that exceeds the tensile strength of dust aggregates consisting of water ice grains with radius $r_0 = 2.38 \pm 1.11 \mu\text{m}$ measured in the laboratory by [Gundlach et al. \(2018\)](#). To correctly understand the size of grains that form planetesimals in protoplanetary discs, therefore, one must seek a remedy against the apparent disagreement between model predictions and measurements of tensile strengths.

In the field of fracture mechanics, it is well-known that the tensile strength of porous media such as snow, ice, aerogels, minerals, and rocks is weakly dependent on the volume of the media (e.g. [Sommerfeld 1974](#); [Petrovic 2003](#); [Patil et al. 2017](#); [Nakamura et al. 2015](#)). However, numerical simulations by both [Seizinger, Speith & Kley \(2013\)](#) and [Tatsuuma et al. \(2019\)](#) dismissed the idea that the tensile strength of dust aggregates depends on the number of monomers, namely, the volume of dust aggregates. Here, we cannot help but wonder if the authors of numerical studies failed to notice the volume effect on the tensile strength of dust aggregates, because the volume effect is so subtle that it easily escapes detection. Therefore, we revisit the tensile strength of dust aggregates to restore the consensus about the size of their constituent grains condensed in protoplanetary discs, by explicitly taking the volume effect into account.

2 TENSILE STRENGTH OF DUST AGGREGATES

The so-called JKR theory provides a rigorous solution for the interaction between elastic spheres characterized by elastic properties of a solid, more precisely, the surface energy γ , Young's modulus E , and Poisson's ratio ν ([Johnson, Kendall & Roberts 1971](#)). [Seizinger et al. \(2013\)](#) and [Tatsuuma et al. \(2019\)](#) performed computer simulations on tensile stress acting on dust aggregates consisting of monodisperse spherical monomers based on the discrete element method (DEM) with the JKR theory. Since theoretical studies on the tensile strength of dust aggregates have been pursued for more than a century, we shall make full use of an analytical model for the tensile strength of dust aggregates based on the JKR theory of contact mechanics and the Griffith theory of fracture mechanics (e.g. [Hertz 1881](#); [Griffith 1921](#); [Rumpf 1970](#); [Kendall 1987](#)). The tensile strength σ of a dust aggregate consisting of spherical monomers with the coordination number n_c may be given by ([Kendall 1987](#); [Kendall & Stainton 2001](#); [Bika, Gentzler & Michaels 2001](#))

$$\sigma = \phi^\beta n_c \gamma r_0^{-1} \epsilon^{-1/2}, \quad (1)$$

where ϕ and ϵ denote the volume filling factor of the aggregate and the ratio of the maximum flaw size to the diameter of the monomers, respectively. Note that equation (1) reduces to [Rumpf's](#) classical formula if $\beta = 1$ and $\epsilon = (4/3)^6$, and to [Kendall's](#) formula if $\beta = 2$ and $n_c = 17.5 \phi^2$ ([Rumpf 1970](#); [Kendall 1987](#)). Hereafter we limit our study to dust aggregates of small elastic grains whose compositions are relevant to primitive dust in protoplanetary discs such as water ice, silicates, and organics.

The tensile strength of an aggregate is known to scale with the volume V of the aggregate as $\sigma \propto V^{-1/m}$ where m is commonly referred to as the Weibull modulus (cf. [Carpinteri 1994](#); [Petrovic 2003](#)). Accordingly, we may rewrite equation (1)

in the following form:

$$\sigma = \left(\frac{4\pi N}{3}\right)^{1/m} \epsilon^{-1/2} \phi^{\beta-1/m} n_c \gamma r_0^{3/m-1} V^{-1/m}, \quad (2)$$

where N is the number of monomers in the aggregate. We may regard $(4\pi N/3)^{1/m} \epsilon^{-1/2}$ in equation (2) to be a constant, because the condition $\epsilon \propto N^{2/m}$ holds for a power-law distribution of flaw sizes (Housen & Holsapple 1999; Carpinteri & Puzzi 2007).

The Weibull modulus m is known to be material dependent, although $m = 6$ is expected for the fully cracked state, in which the average distance between flaws is equal to the flaw size (Housen & Holsapple 1999; Nakamura et al. 2015). Hereafter, we shall assume the Weibull modulus m to be $m = 5$ for water ice, $m = 8$ for siliceous material, and $m = 6$ for carbonaceous matter, by taking into account the literature values of $m \approx 5$ for water ice, $m = 6$ – 10 for amorphous silica, and $m = 6.2$ for amorphous diamond-like carbon (Petrovic 2003; Klein 2009; Borrero et al. 2010).

To examine whether or not outcomes of computational simulations as well as laboratory experiments are reproduced by equation (2), we need a relationship between n_c and ϕ . In general, the coordination number n_c increases with the volume filling factor ϕ , although there is no consensus on the formula to describe the relationship (see van Antwerpen et al. 2010, for a review). For simplicity, we shall use the following relationship between n_c and ϕ :

$$n_c = c_1 \exp(d_1 \phi), \quad (3)$$

where $c_1 = 2.0$ and $d_1 = 2.4$ were determined by Meissner, Michaels & Kaiser (1964).

3 COMPARISON TO AVAILABLE DATA ON THE TENSILE STRENGTH OF DUST AGGREGATES

3.1 Computer simulations

3.1.1 Aggregates of spheres

On the basis of their DEM simulations, Tatsuuma et al. (2019) proposed that the tensile strength σ of porous dust aggregates consisting of N identical spherical monomers is given by the following empirical formula:

$$\sigma = \sigma_0 \left(\frac{\gamma}{0.1 \text{ J m}^{-2}}\right) \left(\frac{r_0}{0.1 \text{ }\mu\text{m}}\right)^{-1} \left(\frac{\phi}{0.1}\right)^\beta, \quad (4)$$

with $\sigma_0 = 9.51$ kPa and $\beta = 1.8$, regardless of N . By the same token, an empirical formula for the tensile strength of porous dust aggregates found by Seizinger et al. (2013) corresponds to $\sigma_0 = 4.43$ kPa and $\beta = 1.88$ in their DEM simulations. One might attribute the difference in the σ_0 and β values of the empirical formula between these two groups to the uncertainty of the results by DEM simulations. Here, we suppose that the results of Tatsuuma et al. (2019) are more accurate, compared with those of Seizinger et al. (2013), according to the magnitude of smaller time steps used in the former than the latter. Tatsuuma et al. (2019) fixed the number of monomers to $N = 2^{14}$ and the volume of the aggregate varies with the volume filling factor ϕ , while Seizinger et al. (2013) fixed the volume to $V = 7.5 \times 10^{-14} \text{ m}^3$ and the number of monomers varies with ϕ . If we consider an aggregate with $r_0 = 0.6 \text{ }\mu\text{m}$ and $\phi = 0.19765$, then we have $N = 2^{14}$ and $V = 7.5 \times 10^{-14} \text{ m}^3$ in both Tatsuuma et al. (2019) and Seizinger et al. (2013). By inserting $r_0 = 0.6 \text{ }\mu\text{m}$, $\phi = 0.19765$, and $\gamma = 0.02 \text{ J m}^{-2}$ into equation (4), we obtain $\sigma = 1.14$ kPa for the former ($\sigma_0 = 10$ kPa, $\beta = 1.8$) and $\sigma = 0.532$ kPa for the latter ($\sigma_0 = 4.43$ kPa, $\beta = 1.88$). Accordingly, we may consider that the tensile strengths of dust aggregates determined in the DEM simulations by Seizinger et al. (2013) are underestimated by a factor of 2.

What follows is the best fit of equation (2) to numerical results of tensile strengths by Tatsuuma et al. (2019) with $\gamma = 0.1 \text{ J m}^{-2}$, $r_0 = 0.1 \text{ }\mu\text{m}$, and $N = 2^{14}$:

$$\sigma = 8 \text{ kPa} \left(\frac{\gamma}{0.1 \text{ J m}^{-2}}\right) \left(\frac{r_0}{0.1 \text{ }\mu\text{m}}\right)^{3/m-1} \left(\frac{\phi}{0.1}\right)^{\beta-1/m} \exp\left[\alpha \left(\frac{\phi}{0.1} - 1\right)\right] \left(\frac{V}{686 \text{ }\mu\text{m}^3}\right)^{-1/m}, \quad (5)$$

with $\beta = 1.5$ and $\alpha = 0.24$, implying $\epsilon = 10^2$ for $N = 2^{14}$. It should be noted that equation (5) cannot be in principle applied to highly compact aggregates of $\phi \gtrsim 0.74$, because the maximum value of volume filling factor for aggregates of spherical monomers is $\phi = \sqrt{2}\pi/6$ (Kepler 1611). The top panels of Fig. 1 demonstrate that equation (5; the solid lines) fairly well reproduces numerical results of Tatsuuma et al. (2019, the filled circles) as well as their empirical formula of equation (4; the dashed lines), irrespective of the values assumed for monomer radius r_0 and surface energy γ . These results validate equation (5) as a substitute for equation (4), which has been formulated by Tatsuuma et al. (2019) for their numerical simulations.

Seizinger et al. (2013) was ahead of Tatsuuma et al. (2019) concerning DEM-based numerical studies on the tensile strength of porous dust aggregates consisting of monodisperse spherical monomers. DEM simulations performed by Seizinger et al. (2013) are based on the JKR theory, although adhesion of monomers to two plates, in which the aggregates are sandwiched, was artificially increased by a factor κ . They investigated how the tensile strength of the aggregates varies with the volume filling factor and the volume of the aggregates as well as the radius of monomers. The left bottom panel of Fig. 1 shows that

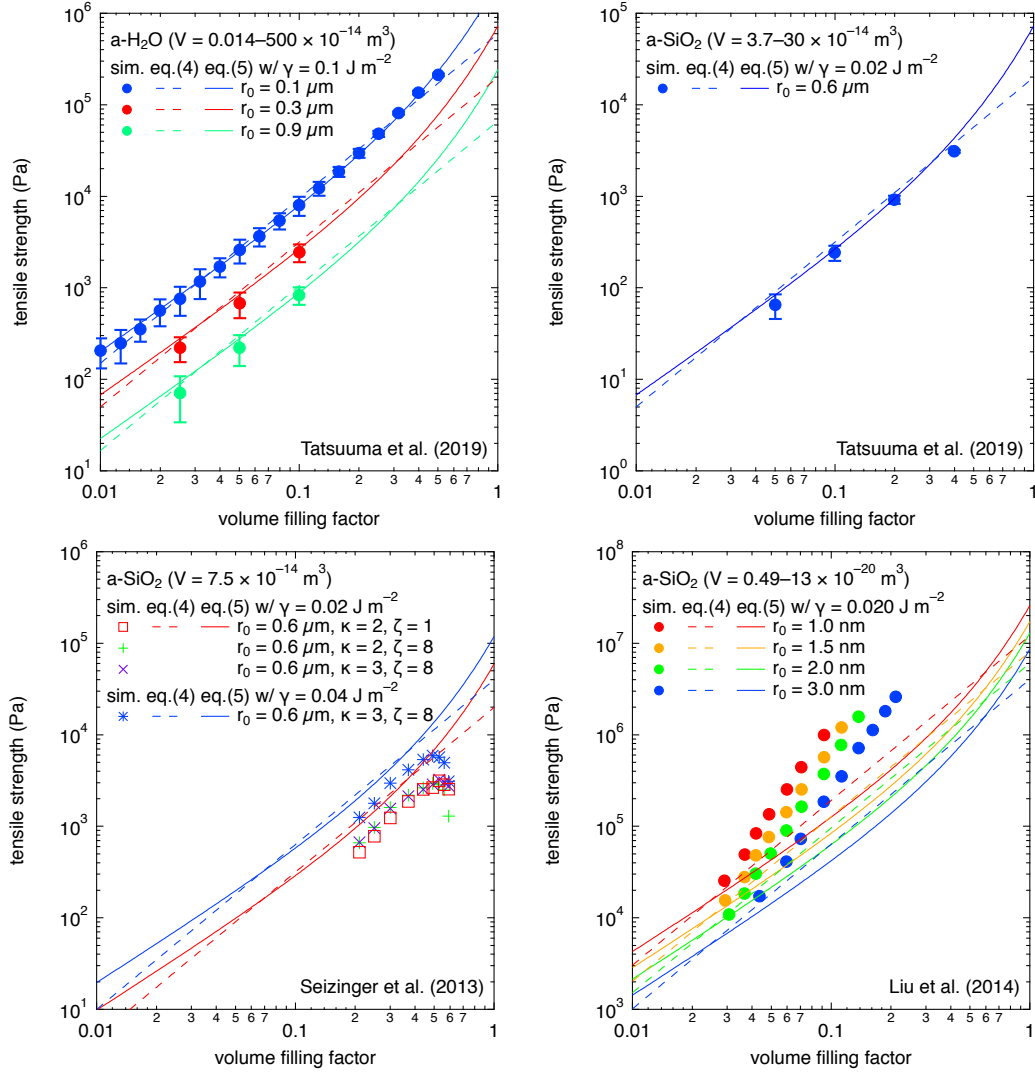


Figure 1. A comparison of tensile strength for porous dust aggregates of monodisperse spherical monomers between DEM simulations and our formula. The symbols: computer simulations; the dashed lines: equation (4); the solid lines: equation (5). Top: simulations based on the JKR theory with $\gamma = 0.1 \text{ J m}^{-2}$ (left) and $\gamma = 0.02 \text{ J m}^{-2}$ (right) by [Tatsuuma et al. \(2019\)](#); left bottom: simulations based on the JKR theory with $\gamma = 0.02$ and $\gamma = 0.04 \text{ J m}^{-2}$ by [Seizinger et al. \(2013\)](#) where κ and ζ denote their so-called wall-glueing factor and rolling modifier; right bottom: DEM simulations based on a combination of the JKR theory and the DMT theory by [Liu et al. \(2014\)](#).

equation (5) predicts the tensile strength of dust aggregates that exceeds the numerical results of [Seizinger et al. \(2013\)](#) by a factor of 2, similar to equation (4), but provides slightly better fits to the results than equation (4) does.

DEM-based numerical studies by [Liu et al. \(2014\)](#) utilized a generalized model for the contact of elastic solids proposed by [Schwarz \(2003\)](#), which incorporates a short-range force in the JKR theory and a long-range force in the DMT theory. We assume the predominance of long-range forces on tensile stress and thus take 3/4 times the long-range component of surface energy to interpret their results in the framework of the JKR theory. As plotted in the right bottom panel of Fig. 1, the values of tensile strength in their results at the smallest volume filling factors appear to be on the same order of magnitude as the values predicted by equation (5), while the deviations grows with the volume filling factor of the aggregates. The dependences of tensile strength on the volume filling factor and the monomer's radius are also stronger in the DEM simulations by [Liu et al. \(2014\)](#) than those by [Tatsuuma et al. \(2019\)](#) and [Seizinger et al. \(2013\)](#) (cf. the top and left-bottom panels of Fig. 1). The strong dependence of tensile strength on the volume filling factor in [Liu et al. \(2014\)](#) most likely originates from an increasing contribution of short-range forces for compact aggregates, because the contribution of short-range forces to tensile stress should increase with the volume filling factor.

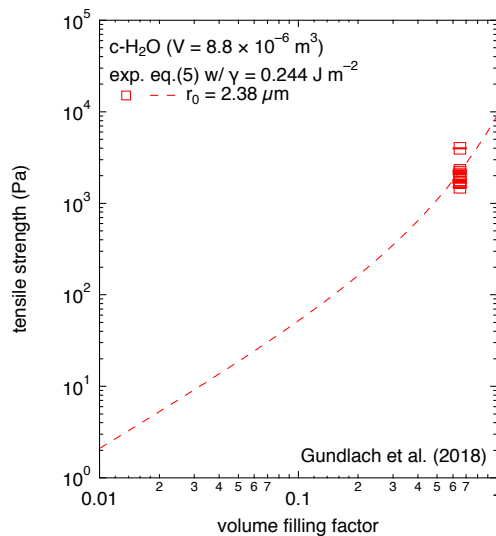


Figure 2. A comparison of tensile strength for dust aggregates of monodisperse spherical ice monomers between laboratory experiments and our formula. The open squares: experimental data for crystalline water ice in air by Gundlach et al. (2018); the dashed line: equation (5) with $\gamma = 0.244 \text{ J m}^{-2}$ for crystalline water ice.

3.2 Laboratory experiments

3.2.1 Water ice

Gundlach et al. (2018) measured the tensile strength of compact dust aggregates consisting of polydisperse spherical water ice particles with $r_0 = 2.38 \pm 1.11 \mu\text{m}$ at a temperature of 150 K in air. They produced crystalline water ice particles by spraying water droplets into liquid nitrogen and formed porous dust aggregates by pressing the monomers into a cylinder. We shall first compare equation (5) to the tensile strengths measured by Gundlach et al. (2018), which were found to be much lower than equation (4) by Tatsuuma et al. (2019). Throughout the paper, we assume $\gamma = 0.244 \text{ J m}^{-2}$ for the surface energy of crystalline water ice Ih derived from the density-functional theory (DFT), although the value may differ by 20%, depending on the crystal face (Pan et al. 2010). Figure 2 shows that equation (5) agrees with laboratory experiments on the tensile strengths of dust aggregates composed of crystalline water ice, dissimilar to equation (4) proposed by Tatsuuma et al. (2019). This demonstrates that the volume effect on the tensile strength incorporated in equation (5) provides a remedy for the discrepancy between laboratory experiments and model predictions.

3.2.2 Silicates

Blum & Schräpler (2004) and Blum et al. (2006) used amorphous silica “sicastar[®]” particles with radius $r_0 = 0.76 \mu\text{m}$ produced by micromod Partikeltechnologie GmbH to form porous ($\phi \approx 0.15\text{--}0.33$) dust aggregates. They uni-axially compressed the aggregates of monodisperse spheres to a pressure of $(4 \pm 2) \times 10^3 \text{ Pa}$ prior to their measurements of tensile strength at medium vacuum conditions ($\sim 100 \text{ Pa}$). Blum et al. (2006) also produced compact ($\phi = 0.41\text{--}0.66$) dust aggregates of monodisperse sicastar[®] spheres by applying an omnidirectional pressure to the aggregates. We assume $\gamma = 0.150 \text{ J m}^{-2}$ for the surface energy of sicastar[®] (micromod Partikeltechnologie GmbH), which is consistent with collision experiments using sicastar[®] spheres (cf. Kimura et al. 2015). The left top panel of Fig. 3 shows that the experimental data for the tensile strength of porous and compact aggregates obtained by Blum & Schräpler (2004) and Blum et al. (2006) are reasonably in good harmony with equation (5) if $\gamma = 0.150 \text{ J m}^{-2}$. It should be noted that equation (5) shows to some extent deviations from experimental data on the tensile strength of compact dust aggregates with large ϕ values.

Gundlach et al. (2018) measured the tensile strength of compact dust aggregates consisting of monodisperse sicastar[®] spheres at room temperature in air. Since they formed compact dust aggregates by pressing the monomers into a cylinder, we consider that monomers are in contact without help of adsorbed water molecules on their surfaces (i.e. $\gamma = 0.150 \text{ J m}^{-2}$). The right top of Fig. 3 compares equation (5) with their laboratory experiments on the tensile strengths of dust aggregates composed of amorphous silica. The tensile strength of compact dust aggregates consisting of amorphous silica monomers with $r_0 = 0.15 \mu\text{m}$ measured in air by Gundlach et al. (2018) is higher than equation (5) with $\gamma = 0.150 \text{ J m}^{-2}$, although their results with $r_0 = 0.50$ and $0.75 \mu\text{m}$ are in good agreement with equation (5).

Steinpilz et al. (2019) also used sicastar[®] to form compact dust aggregates of silica spheres with $r_0 = 0.6 \mu\text{m}$ by pressing

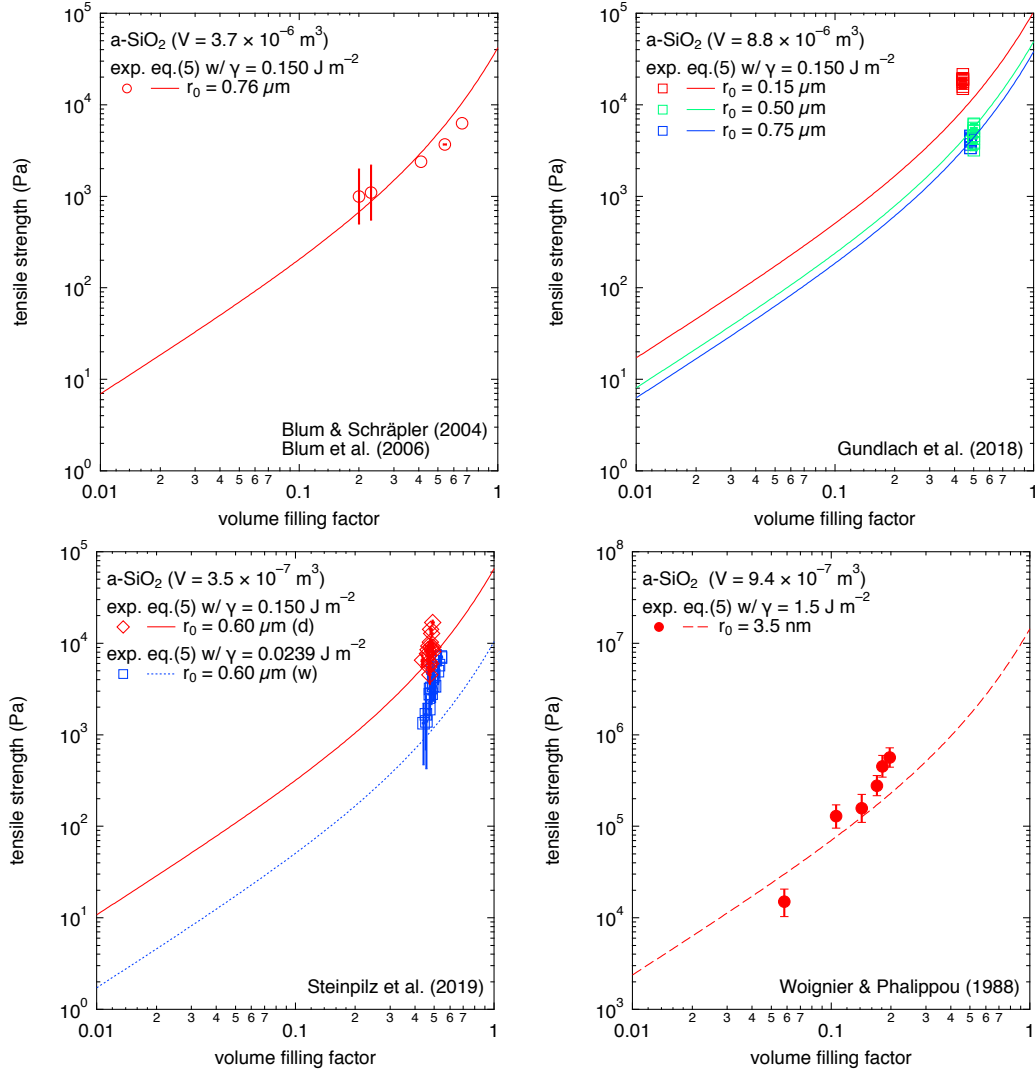


Figure 3. A comparison of tensile strength for dust aggregates of monodisperse and polydisperse spherical silica monomers between laboratory experiments and our formula. The solid lines: equation (5) with $\gamma = 0.150 \text{ J m}^{-2}$ for sicastar[®] silanol-bonded silica in vacuum or high temperature; the dashed line: equation (5) with $\gamma = 1.5 \text{ J m}^{-2}$ for siloxane-bonded amorphous silica; the dotted line: equation (5) with $\gamma = 0.0239 \text{ J m}^{-2}$ for hydrated amorphous silica in air. The open circles (left top): experimental data for porous and compact aggregates of amorphous silica measured in vacuum by Blum & Schr apler (2004) and Blum et al. (2006); the open squares (right top): experimental data for amorphous silica in air by Gundlach et al. (2018); the open squares (left bottom): experimental data for compact aggregates of wet (w), unheated amorphous silica measured in air by Steinpilz, Teiser & Wurm (2019); the open diamonds (left bottom): experimental data for compact aggregates of dry (d), heated amorphous silica measured in air by Steinpilz et al. (2019); the filled circles (right bottom) experimental data for amorphous silica in air by Woignier & Phalippou (1988).

the aggregates up to a pressure of $5.5 \times 10^4 \text{ Pa}$ ¹. They measured the tensile strength of compact aggregates at room temperature in air before and after heating to 250°C for 24 hrs in the oven. Because of its hydrophilic nature, amorphous silica particles in air are known to swell with adsorbed water molecules and the surface energy of amorphous silica is reduced typically to $\gamma \sim 0.0239 \text{ J m}^{-2}$ at room temperature (Kendall, Alford & Birchall 1987). Therefore, evaporation of water molecules by heating to higher temperatures elevates the surface energy of amorphous silica, in a similar way to vacuum conditions (Maszara et al. 1988; Kimura et al. 2015). By the same token, Kamiya et al. (2002) observed an increase in the tensile strength of amorphous silica powders with temperature, as expected from equation (5), which predicts the proportionality of tensile strength to surface energy. The left bottom panel of Fig. 3 shows that the tensile strengths of unheated and heated compact aggregates are consistent with equation (5) if $\gamma = 0.0239 \text{ J m}^{-2}$ for the former and $\gamma = 0.150 \text{ J m}^{-2}$ for the latter. Note that Steinpilz et al. (2019) corrected the volume filling factor for unheated aggregates by taking into account the apparent reduction in the

¹ Steinpilz et al. (2019) did not explicitly describe the quantity of applied pressures to press their aggregates, but mentioned that they took the same procedure as Meisner, Wurm & Teiser (2012) who gave a pressure of $\lesssim 5.5 \times 10^4 \text{ Pa}$.

volume filling factor due to adsorption of water molecules (cf. Appendix A). This indicates that lower values of volume filling factor correspond to higher amounts of adsorbed water molecules, which are equivalent to lower values of surface energy. Accordingly, their results are consistent with equation (5), because a reduction in the volume filling factor, in turn, the surface energy, is expected to decrease the tensile strength.

The tensile strength of silica aerogels consisting of polydisperse spherical monomers with radius $r_0 = 3.0\text{--}4.0$ nm was measured at room temperature in air by [Woignier & Phalippou \(1988\)](#). Silica aerogels are highly porous dust aggregates and the monomers are strongly bonded by siloxane (Si–O–Si) bridges, although silanol (Si–OH) groups may remain on the outside. Therefore, we may apply the value of $\gamma = 1.5$ J m⁻² to the surface energy of silica aerogels in equation (5), irrespective of vacuum conditions, while the value of γ for amorphous silica with siloxane bonding is uncertain within a factor of 2 (see [Kimura et al. 2015](#)). The right bottom panel of Fig. 3 proves that the tensile strength of dust aggregates given by equation (5) is applicable to highly porous silica aerogels within a factor of 2, although the dependence of tensile strength on the volume filling factor of dust aggregates appears to be slightly steeper in experiments, compared with equation (5).

[Blum et al. \(2006\)](#) measured the tensile strengths of porous ($\phi = 0.13$) dust aggregates consisting of polydisperse irregularly shaped silica particles with $r_0 = 1.25^{+3.75}_{-1.20}$ μm at medium vacuum conditions (~ 100 Pa). [Meisner et al. \(2012\)](#) prepared more compact ($\phi = 0.37\text{--}0.51$) dust aggregates of polydisperse irregularly shaped silica particles with $r_0 = (1.5 \pm 1.0)$ μm by applying an omnidirectional pressure of $\lesssim 5.5 \times 10^4$ Pa to the aggregates. They applied the Brazilian test, which is one of the most popular indirect tensile tests, to measure the tensile strength of the aggregates in a vacuum chamber at medium vacuum conditions of $\lesssim 4$ Pa. We consider $\gamma = 0.243$ J m⁻² to best represent the surface energy of amorphous silica in vacuum, since the surface tension of silica glass asymptotically approaches this value at absolute zero ([Kimura et al. 2020](#)). As shown in the top panels of Fig. 4, equation (5) with $\gamma = 0.243$ J m⁻² reproduces the tensile strengths of both porous (left) and compact (right) aggregates consisting of irregularly shaped silica particles. The Brazilian test with highly compact ($\phi = 0.64\text{--}0.78$) dust aggregates of polydisperse irregularly shaped silica particles was conducted by [San Sebastián et al. \(2020\)](#). While the tensile strength of the aggregates was measured at atmospheric conditions, the influence of adsorbed water molecules on the surface of silica particles is most likely negligible for such compact aggregates formed by intense compression prior to the measurements. Therefore, we compare their experimental results to equation (5) with $\gamma = 0.243$ J m⁻², which is shown in the middle panel of Fig. 4. The good fit of the experimental data to the theoretical curve justifies the validity of equation (5) within the expected range of volume filling factor for dust aggregates, namely, $\phi < 0.8$.

[Jimbo et al. \(1968\)](#) and [Naito et al. \(1986\)](#) measured the tensile strength of granular materials consisting of polydisperse irregularly shaped silica sand with radii $r_0 = 2, 2.15, 5,$ and 6 μm . [Jimbo et al. \(1968\)](#) prepared their silica powder beds by either tapping or compression in the range of $5.0 \times 10^2\text{--}5.0 \times 10^4$ Pa, but the tensile strength did not strongly depend on the method of sample preparation as shown in Fig. 4. They determined adhesion forces of the same silica sand powders to flat plates using centrifugal forces, which results in $\gamma = 0.050$ J m⁻² ([Asakawa & Jimbo 1967](#))². Therefore, we consider that the value of $\gamma = 0.050$ J m⁻² is appropriate to the surface energy of quartz used in their experiments, while $\gamma = 1.5$ J m⁻² for quartz in vacuum (see Appendix B for the surface energy of quartz). Indeed, their results on the tensile strength of silica sand powder beds are consistent with equation (5) if $\gamma = 0.050$ J m⁻², as shown in the left bottom panel of Fig. 4.

[Takahashi et al. \(1979\)](#) heated silica sand of $r_0 = 1.6$ μm at a temperature of $110\text{--}150^\circ\text{C}$ for 48 hrs in air and kept the powders in a desiccator for more than a day prior to their experiments. It is well-known that the surface energy of crystalline silica (i.e. quartz) increases with temperature, owing to evaporation of water molecules and the formation of siloxane bonding (e.g. [Parks 1984](#)). By applying high pressures of $9.8 \times 10^4\text{--}9.8 \times 10^7$ Pa to their fine powder beds, they prepared compact powder beds of irregularly shaped quartz particles. They found a gradual increase of tensile strength with pressure up to 4.9×10^7 Pa, but no more increase above 4.9×10^7 Pa. The right bottom panel of Fig. 4 shows that their results are in harmony with equation (5) if $\gamma = 1.5$ J m⁻². It should be noted that the surface energy of $\gamma \approx 1.5$ J m⁻² suggests siloxane bonding, which corresponds to the surface chemistry of quartz in vacuum. Therefore, we attribute their results of high tensile strengths for highly compressed, heated powder beds to the achievement of siloxane bonding between monomers (see, e.g. [Stengl, Tan & Gösele 1989](#)).

3.2.3 Organic matter

To the best of our knowledge, astronomically relevant carbonaceous matter has not been utilized for tensile strength measurements of dust aggregates. Accordingly, we shall substitute lactose for astronomical organic matter, by taking into account the availability of tensile strength measurements for granular materials of lactose in air. The surface energy of crystalline α -lactose with a lack of surface contamination was measured to be $\gamma = 0.217$ and 0.129 J m⁻² for crystalline α -lactose anhydrous and crystalline α -lactose monohydrate, respectively ([Traini et al. 2008](#); [Das et al. 2009, 2010](#); [Jones, Young & Traini 2012](#)). It is

² [Asakawa & Jimbo \(1967\)](#) derived an average adhesive force of $F_{\text{ad}} = 3.9 \times 10^{-6}$ N from their measurements with silica sand powders of the mean radius $r_0 = 8.25$ μm . By applying the JKR theory (i.e. $F_{\text{ad}} = 3\pi\gamma r_0$) to their measurements, one could obtain the surface energy of $\gamma = 0.050$ J m⁻².

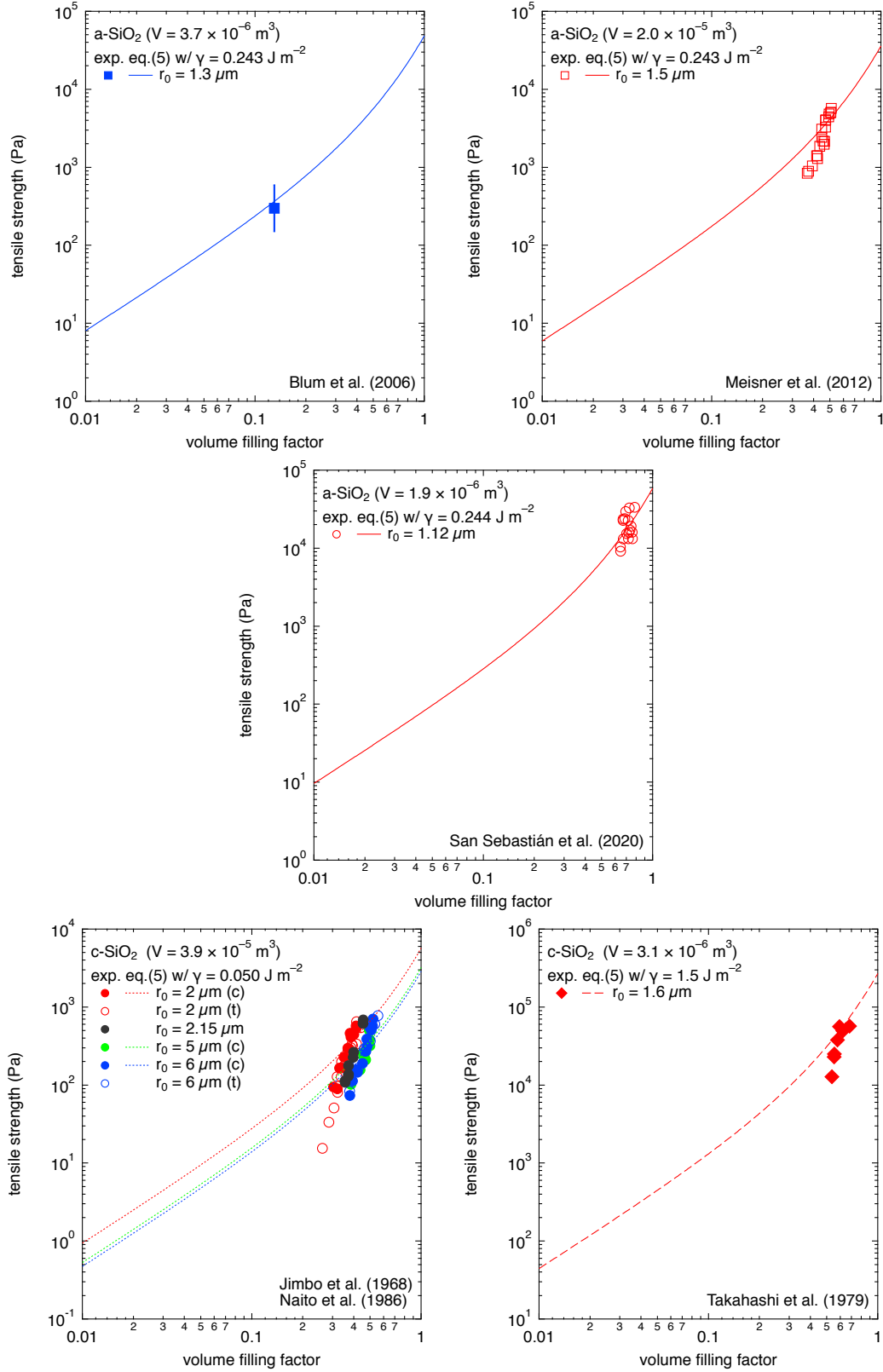


Figure 4. A comparison of tensile strength for porous and compact dust aggregates of polydisperse irregularly shaped silica monomers between laboratory experiments and our formula. Left top: porous aggregates of amorphous silica in vacuum by Blum et al. (2006, the filled squares); right top: mildly compact aggregates of amorphous silica in air by Meisner et al. (2012, the open squares); middle: highly compact aggregates of amorphous silica in air by San Sebastián et al. (2020, the open circles); left bottom: silica sand powder beds prepared by compression (c) or tapping (t) in air by Jimbo, Asakawa & Soga (1968) and Naito et al. (1986, the open and filled circles); right bottom: silica sand powder beds prepared by heating and strong compression in air by Takahashi et al. (1979, the filled diamonds); the solid lines: equation (5) with $\gamma = 0.243 \text{ J m}^{-2}$ for amorphous silica and equation (5) with $\gamma = 0.050 \text{ J m}^{-2}$ or $\gamma = 1.5 \text{ J m}^{-2}$ for crystalline silica.

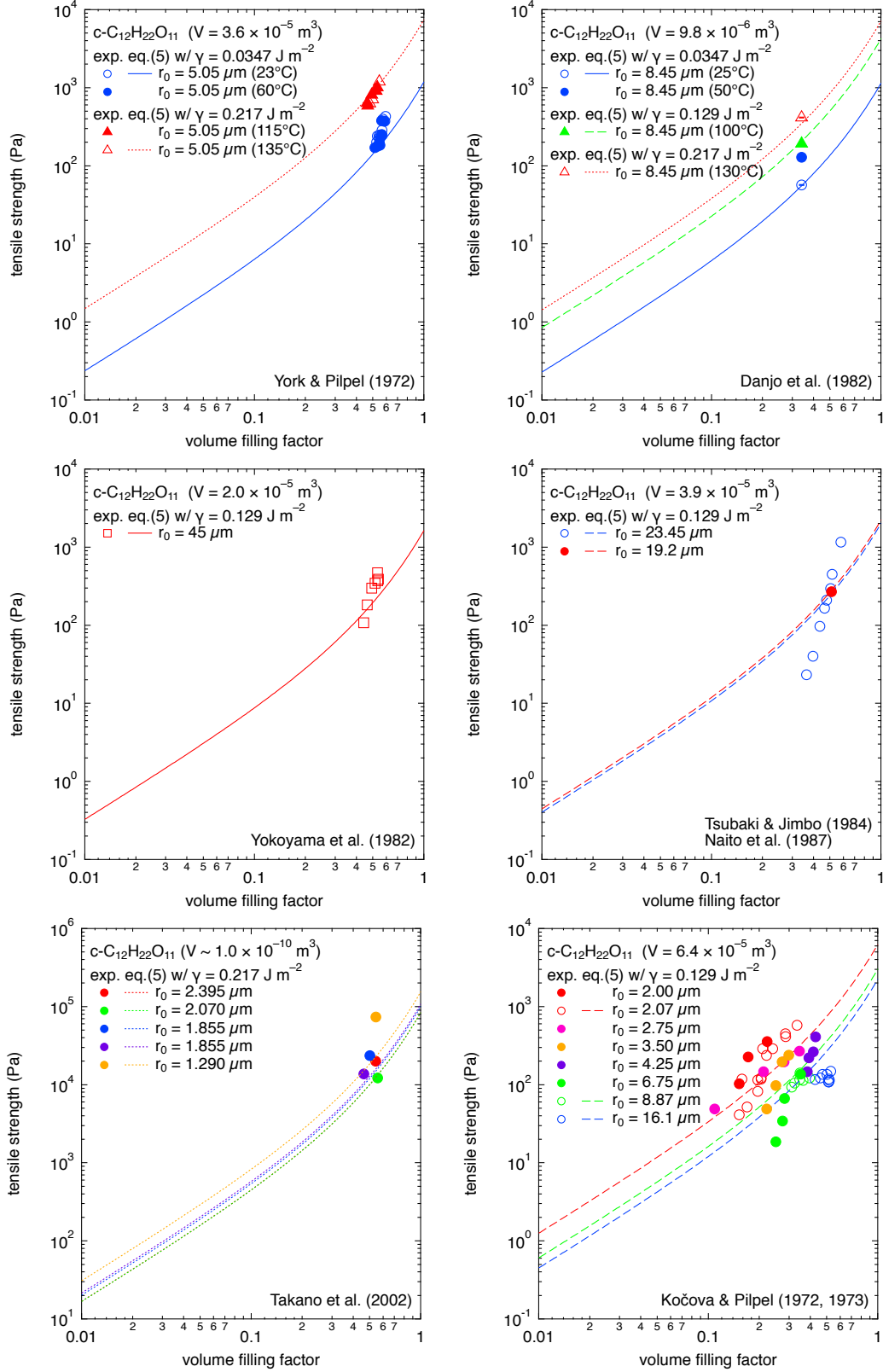


Figure 5. A comparison of tensile strength for granular materials of polydisperse irregularly shaped lactose monomers between laboratory experiments in air by York & Pilpel (1972, left top), Danjo, Iida & Otsuka (1982, right top); Yokoyama, Fujii & Yokoyama (1982, left middle); Tsubaki & Jimbo (1984) and Naito et al. (1987, right middle), Takano et al. (2002, left bottom), and Kočova & Pilpel (1972), Kočova & Pilpel (1973, right bottom) and our formula. The open and filled circles: experimental data for lactose powder beds at room temperature; the open and filled triangles: experimental data for lactose powder beds at slightly elevated temperature; the solid lines: equation (5) with $\gamma = 0.0347 \text{ J m}^{-2}$; the dotted line: equation (5) with $\gamma = 0.217 \text{ J m}^{-2}$.

well-known that lactose is hydrophilic and the surface of lactose at room temperature in air is easily covered by adsorbed water molecules, which reduce the surface energy. The surface energy of crystalline α -lactose monohydrate determined by [Sindel & Zimmermann \(2001\)](#) using atomic force microscopy (AFM) was $\gamma = 0.0347 \text{ J m}^{-2}$ at room temperature in air³.

[York & Pilpel \(1972\)](#) studied experimentally how the tensile strength of crystalline α -lactose monohydrate powders with $r_0 = 5.05 \text{ }\mu\text{m}$ varies with temperature of the powders. Their results⁴ show that the tensile strength of the powders is constant in the range of temperature from 23 to 60°C, and elevated from 90 to 160°C. The left top panel of Fig. 5 shows their measurements on the tensile strength of polydisperse irregularly shaped lactose powders and equation (5) with $\gamma = 0.0347 \text{ J m}^{-2}$ (the solid line) and $\gamma = 0.217 \text{ J m}^{-2}$ (the dotted line) as a function of the volume filling factor at room temperature as well as at elevated temperatures. The experimental data at temperatures of 115 and 135°C are situated on the dotted line of equation (5) with $\gamma = 0.217 \text{ J m}^{-2}$, consistent with thermal dehydration of monohydrate lactose around 120°C (see [Danjo et al. 1982](#)).

[Danjo et al. \(1982\)](#) confirmed the temperature effect on the tensile strength of polydisperse irregularly shaped crystalline α -lactose monohydrate powders with $r_0 = 8.45 \text{ }\mu\text{m}$ in air. Their data shown in the right top panel of Fig. 5 and in harmony with equation (5) are obtained after they attained the selected temperatures in 30 minutes and then kept the temperatures for 4.5 h.

[Yokoyama et al. \(1982\)](#) prepared a powder bed of polydisperse lactose particles with $r_0 = 45 \text{ }\mu\text{m}$ by pressing the sample until the thickness of the powder bed reaches 10 mm. The authors did not describe which form of lactose was used in their experiments, while we assume crystalline α -lactose monohydrate that is the most common form of lactose at room temperature in air ([Carpin et al. 2016](#)). Since the compressed powder beds remained compact for 10 minutes as reported by the authors, we consider that the effect of adsorbed water molecules on the cohesion of particles is minimized for their samples. Therefore, we may regard $\gamma = 0.129 \text{ J m}^{-2}$ as the most appropriate value of surface energy for their powder beds, when comparing equation (5) with their experimental data obtained at room temperature in air. The left middle panel of Fig. 5 shows that equation (5) with $\gamma = 0.129 \text{ J m}^{-2}$ reasonably reproduces their experimental data.

[Tsubaki & Jimbo \(1984\)](#) presented their experimental data for the tensile strength of polydisperse α -lactose monohydrate powders with $r_0 = 23.45 \text{ }\mu\text{m}$ measured at room temperature in air. They pressed their powder beds prior to measurements and found that the tensile strength increases with the pre-compressive stress, which controls the volume filling factor of the powder beds. [Naito et al. \(1987\)](#) measured the tensile strength of polydisperse irregularly shaped α -lactose monohydrate powders with $r_0 = 19.2 \text{ }\mu\text{m}$ at a temperature of 20°C and a relative humidity of 50%. While the former prepared their powder beds by compression in the range of 0.5×10^3 – $1 \times 10^5 \text{ Pa}$, the latter 1.55×10^3 – $11.5 \times 10^3 \text{ Pa}$. Their powder beds were prepared in the same volume and thus their results are plotted together in the right middle panel of Fig. 5. The coincidence of equation (5) with their results of tensile strength is fairly good, although the compression during the sample preparation seems to affect the tensile strength.

The tensile strength of nearly spherical compact aggregates composed of polydisperse crystalline lactose particles was measured by [Takano et al. \(2002\)](#) in the ranges of volume from $V = 2.7 \times 10^{-11}$ to $2.6 \times 10^{-10} \text{ m}^3$, depending on the radius of monomers. Since a special type of dry granulation, referred to as pressure swing granulation (PSG), was utilized for milled α -lactose particles to tightly agglomerate together, lactose particles are in contact without help of adsorbed water molecules on their surfaces. Therefore, we may adopt $\gamma = 0.248 \text{ J m}^{-2}$ for nearly spherical compact dust aggregates consisting of polydisperse crystalline lactose monomers produced by the PSG method. The experimental values of tensile strength are scattered around equation (5), but the result for the aggregates consisting of the smallest monomers with $r_0 = 1.29 \text{ }\mu\text{m}$ greatly exceeds the tensile strength expected from equation (5).

[Kořova & Pilpel \(1972, 1973\)](#) used irregularly shaped polydisperse powders of crystalline α -lactose monohydrate with $r_0 = 2.00, 2.07, 2.75, 3.50, 4.25, 6.75, 8.87, 16.1 \text{ }\mu\text{m}$ for their measurements of tensile strength at room temperature in air. Since they performed their measurement with a dehumidifier after the powders were dried at a temperature of 105°C, we may

³ [Sindel & Zimmermann \(2001\)](#) measured a pull-off force F of lactose surfaces using a lactose particle as a tip of their AFM cantilever. Since the pull-off force F_{ad} and the radius R_{tip} of the tip were determined to be $F_{\text{ad}} = 5.0 \pm 3.06 \text{ nN}$ and $R_{\text{tip}} = 15.3 \text{ nm}$, respectively, we obtain $\gamma = 0.0347 \pm 0.0212 \text{ J m}^{-2}$ for the surface energy of α -lactose monohydrate at room temperature in air. We are aware that [Zhang et al. \(2006\)](#) derived $\gamma = 0.0233 \pm 0.0023 \text{ J m}^{-2}$ for α -lactose monohydrate from their AFM measurements with a silica tip at room temperature in air. Here, they assumed $\gamma = 0.042 \text{ J m}^{-2}$ for silica to derive the surface energy of lactose from their measurements of $F_{\text{ad}} = 6.34 \pm 0.35 \text{ nN}$ with $R_{\text{tip}} = 21.6 \pm 0.6 \text{ nm}$. It should be, however, noted that the surface energy of silica is strongly environmental dependent at room temperature in air and thus the assumption of $\gamma = 0.042 \text{ J m}^{-2}$ for their silica tip cannot be justified ([Kimura et al. 2015](#)). Using an AFM from the same manufacture as [Zhang et al. \(2006\)](#), [Bérard et al. \(2002\)](#) obtained $F_{\text{ad}} = 31 \text{ nN}$ for α -lactose monohydrate at room temperature in air with a silica cantilever of $R_{\text{tip}} = 20 \text{ nm}$. The large discrepancy between the two results of pull-off force cannot be accounted for by the difference in the size of the tips, but most probably by the difference in the surface energy of the tips.

⁴ The tensile strength of crystalline α -lactose monohydrate powders was degraded at 180°C, which may be attributed to thermal degradation of lactose, because pyrolysis of lactose takes place between 150°C and 200°C ([Hohno & Adachi 1982](#)). Therefore, we shall disregard their experimental results on the tensile strength of α -lactose powders obtained at temperatures higher than 150°C.

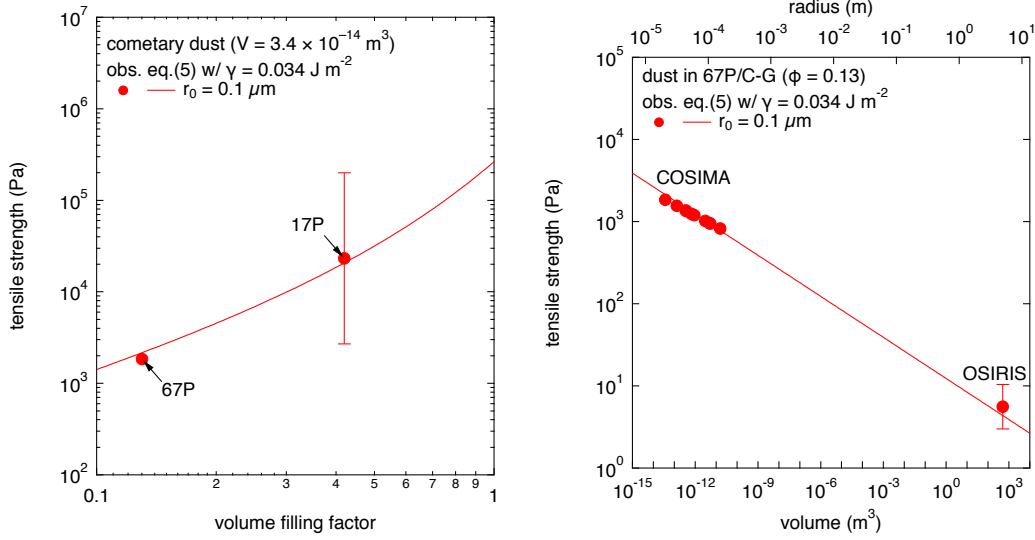


Figure 6. A comparison of tensile strength between cometary dust (the filled circles) and porous dust aggregates of monodisperse spherical monomers in our formula with $r_0 = 0.1 \mu\text{m}$ and $\gamma = 0.034 \text{ J m}^{-2}$ (the solid lines). Left: dust particles with radius $R = 20 \mu\text{m}$ in the comae of 17P/Holmes and 67P/Churyumov-Gerasimenko. Right: dust particles with volume filling factor $\phi = 0.13$ in the coma and on the surface of 67P/Churyumov-Gerasimenko observed by the COSIMA and OSIRIS instruments onboard Rosetta.

assume $\gamma = 0.129 \text{ J m}^{-2}$ for their dried α -lactose powders. While their results are scattered around equation (5), irrespective of monomer size, there does not seem to show a clear discrepancy between equation (5) and their results.

3.3 Astronomical observations

3.3.1 Cometary dust

Thanks to an explosion on Comet 17P/Holmes, Reach et al. (2010) were able to estimate the tensile strength of dust particles ejected from the surface of the comet. They found that the tensile strength of $\sigma = 23.2_{-20.5}^{+176.8}$ kPa is required to release dust particles with radius $R = 20_{-18}^{+180} \mu\text{m}$. Hornung et al. (2016) estimated the tensile strength of dust particles ejected from 67P/C-G using COSISCOPE images of dust aggregates in the size range of $R = 20\text{--}155 \mu\text{m}$ collected by the Rosetta/COSIMA instrument. COSIMA/Rosetta images and mass spectra of dust aggregates in the coma of 67P/C-G show that the surface chemistry of the aggregates is consistent with carbonization of organic matter characterized by the surface energy of $\gamma = 0.034 \text{ J m}^{-2}$ (Kimura et al. 2020). The left panel of Fig. 6 shows that the tensile strength of dust particles with $R = 20 \mu\text{m}$ is well reproduced by equation (5) with $r_0 = 0.1 \mu\text{m}$ and $\gamma = 0.034 \text{ J m}^{-2}$.

Groussin et al. (2015) derived the tensile strength of overhangs on the surface of 67P/C-G to be $\sigma = 5.6_{-2.6}^{+9.4}$ Pa from Rosetta/OSIRIS images by assuming the length of 10 m and the height of 5 m. Because the size of boulders located at the feet of these overhangs is approximately 10 m, we take 10 m as the width of the overhangs to estimate the volume of the overhangs. OSIRIS images revealed that photometric and spectrophotometric data are best explained by the Hapke’s reflectance model if the volume filling factor of its surface is $\phi = 0.13$ (Fornasier et al. 2015). The right panel of Fig. 6 depicts the tensile strength of dust aggregates for the surface of comet 67P/C-G obtained by COSISCOPE images of dust particles and OSIRIS images of overhangs. This clearly shows the volume effect on the tensile strength for cometary dust aggregates, which is accounted for by equation (5) with $r_0 = 0.1 \mu\text{m}$ and $\gamma = 0.034 \text{ J m}^{-2}$.

3.3.2 Meteor showers

Trigo-Rodríguez & Llorca (2006) determined the tensile strength of cometary meteoroids based on ground-based observations of meteor showers, which suggests an increase in the strength with the density of meteoroids. Since they claim that a typical radius of meteoroids presented in their paper is $r < 5 \text{ mm}$, we consider two apparent radii of $R = 0.1 \text{ mm}$ ($V = 4.2 \times 10^{-12} \text{ m}^3$) and $R = 1.0 \text{ mm}$ ($V = 4.2 \times 10^{-9} \text{ m}^3$). On the basis of a model for quasi-continuous fragmentation of meteoroids, Babadzhanyan & Kokhirova (2008) determined the porosities of meteoroids, which are converted into the volume filling factors ϕ in our study. The left panel of Fig. 7 compares the tensile strength of cometary meteoroids with various ϕ values derived from ground-based observations of meteor showers to equation (5) with $r_0 = 0.1 \mu\text{m}$ and $\gamma = 0.034 \text{ J m}^{-2}$. We find that the tensile strengths of cometary meteoroids are scattered along equation (5) with a radius of $R = 0.1$ and 1.0 mm .

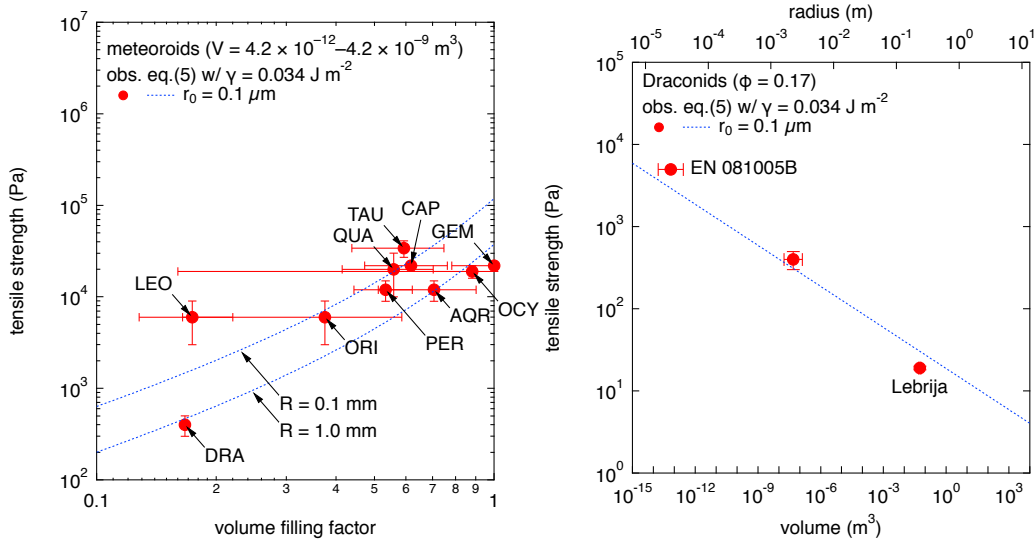


Figure 7. A comparison of tensile strength between cometary meteoroids based on meteor observations (the filled circles) and dust aggregates of monodisperse spherical monomers based on our formula: equation (5) with $r_0 = 0.1 \mu\text{m}$ and $\gamma = 0.034 \text{ J m}^{-2}$. Left: the blue-dotted line: equation (5) with aggregate radii $R = 0.1$ and 1.0 mm; AQR: δ -Aquirids; CAP: α -Capricornids; DRA: Draconids (Giacobinids); GEM: Geminids; LEO: Leonids; OCY: σ -Cygnids; ORI: Orionids; PER: Perseids; QUA: Quadrantids; TAU: Taurids. Right: the blue-dotted line: equation (5) with volume filling factor $\phi = 0.17$; the filled circles: Draconid meteor observations inclusive of EN 081005B and Lebrija Draconid fireballs.

Borovička, Spurný & Koten (2007) derived the tensile strength of $\sigma = 5$ kPa for the EN 081005B Draconid fireball with radius $R = 0.025^{+0.015}_{-0.009}$ mm from its light curve photographed by Super-Schmidt cameras, similar to the precedent study by Trigo-Rodríguez & Llorca (2006). Trigo-Rodríguez & Llorca (2006) estimated the tensile strengths of meteoroids using various observed meteor data inclusive of Fujiwara et al. (2001), from which we obtain $R = 2.25^{+0.90}_{-0.64}$ mm for Draconids by assuming a density of 300 kg m^{-3} . Madiedo et al. (2013) derived the tensile strength of $\sigma = 19 \pm 1$ Pa for an extraordinary bright Draconid fireball ‘Lebrija’ with radius $R = 0.23$ m from their observations at multiple stations. The right panel of Fig. 7 shows the tensile strengths of typical Draconids with $R \approx 0.02$ – 2.0 mm and an extraordinary Draconid fireball of $R \approx 0.2$ m, and equation (5) with $r_0 = 0.1 \mu\text{m}$, $\gamma = 0.034 \text{ J m}^{-2}$, and $\phi = 0.17$. A reasonable fit of equation (5) to observations of Draconids justifies the validity of equation (5) to describe the volume effect on the tensile strength of dust aggregates, although the tensile strengths of the EN 081005B and Lebrija fireballs lie slightly above and below equation (5), respectively.

4 DISCUSSION

We find that equation (5) is capable of reproducing the dependences of tensile strength on the volume filling factor, irrespective of monomer’s composition, size, crystallinity, and surface chemistry. However, we admit that the tensile strength of compact dust aggregates consisting of the smallest sicstar[®] spheres with $r_0 = 0.15 \mu\text{m}$ measured in air by Gundlach et al. (2018) exceptionally exceeds the value expected by equation (5) with $\gamma = 0.150 \text{ J m}^{-2}$ (see the right top panel of Fig. 3). It is worthwhile noting that amorphous silica particles at room temperature in air are known to swell up by adsorption of water molecules, owing to its hydrophilic nature (Vigil et al. 1994; Zhuravlev 2000). Steinpilz et al. (2019) estimated the thickness Δr_0 of water layers on the surface of sicstar[®] to be $\Delta r_0 = (25.3 \pm 4.0)$ nm at atmospheric conditions. It turned out that the smaller the size of monomers is, the stronger the effect of adsorbed water on the volume filling factor of dust aggregates is (see Appendix A). If we assume the same thickness of water molecules for sicstar[®] spheres with $r_0 = 0.15 \mu\text{m}$, then we find that the volume filling factor of compact dust aggregates was $\phi = 0.54$, instead of $\phi = 0.44$. Therefore, the deviation of equation (5) from the experimental data on the tensile strength of compact aggregates with $r_0 = 0.15 \mu\text{m}$ could at least partly be attributed to underestimation of volume filling factors due to water adsorption in laboratory experiments.

Another clear mismatch between experiments and our formula is the tensile strength of PSG lactose granules consisting of polydisperse monomers with $r_0 = 1.29 \mu\text{m}$ produced by Takano et al. (2002) (see the left bottom panel of Fig. 5). Their SEM (Scanning Electron Microscope) images of PSG granules show that the compactness of a granule with $r_0 = 1.29 \mu\text{m}$ is distinct from that with the other monomers’ radii. Because the granule with $r_0 = 1.29 \mu\text{m}$ appears as a single compact sphere in the SEM image, the volume filling factor of the granule could be as high as $\phi \approx 0.78$ (cf. Beck & Volpert 2003). While we cannot rule out model limitations, an underestimation of the volume filling factor for the specific granule may be a remedy for the discrepancy between the experiments and the model.

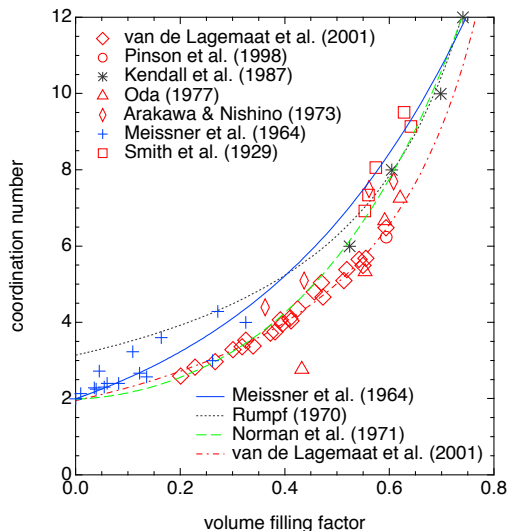


Figure 8. Models of a prescription for the relationship between the coordination number n_c and the volume filling factor ϕ , compared to data on the n_c – ϕ relationship from Smith, Foote & Busang (1929), Meissner et al. (1964), Arakawa & Nishino (1973), Oda (1977), Kendall et al. (1987), Pinson et al. (1998), and van de Lagemaat, Benkstein & Frank (2001). Solid line: Meissner et al. (1964); dotted line: Rumpf (1970); dashed line: Norman, Maust & Skolnick (1971); dash-dotted line: van de Lagemaat et al. (2001).

One may notice in the right bottom panel of Fig. 1 that equation (5) predicts the tensile strength of dust aggregates consisting of monodisperse spherical monomers a factor of two larger than the results of DEM simulations by Seizinger et al. (2013). On closer inspection, however, the right top and left bottom panels of Fig. 1 shows that the tensile strength determined by Seizinger et al. (2013) is smaller by a factor of two compared to Tatsuuma et al. (2019), although they both rely on the JKR theory for dust aggregates with $r_0 = 0.6 \mu\text{m}$ and $\gamma = 0.02 \text{ J m}^{-2}$. One of the noticeable differences in their numerical simulations is a time step for integration; the former uses $1\text{--}3 \times 10^{-10}$ sec, while the latter 1.9×10^{-11} sec. It is most likely that the larger the time steps in DEM simulations are, the higher the possibility of overlooking the maximum tensile stress in the simulations is. Therefore, we conclude that DEM simulations by Seizinger et al. (2013) may be underestimated by a factor of 2, owing to the use of large time steps in their simulations.

We find that equation (5) slightly underestimates and overestimates the tensile strength of the Draconid fireballs ‘EN 081005B’ and ‘Lebrija’, respectively (the right panel of Fig. 7), if we use the volume filling factor of $\phi = 0.17$, according to Babadzhanov & Kokhirova (2008). While Babadzhanov & Kokhirova (2008) estimated the porosity (i.e. the volume filling factor) of Draconids based on the density of 300 kg m^{-3} , Madiedo et al. (2013) suggested a lower density of 100 kg m^{-3} for the Lebrija fireball. Because the tensile strength increases with the density, in other words, the volume filling factor as expressed in equation (5), it is reasonable to attribute the deviation of the Lebrija fireball from our prediction to the low density of the Lebrija fireball. As a result, we cannot rule out the possibility that the density of meteoroids decrease with radius, as inferred for dust particles in the coma of comet 1P/Halley from photopolarimetric properties of the particles (see Lamy, Grün & Perrin 1987). Consequently, equation (5) is still valid for estimating the tensile strength of cometary meteoroids, if we assume $r_0 = 0.1 \mu\text{m}$ and $\gamma = 0.034 \text{ J m}^{-2}$. We should, however, remind the reader that a comprehensive analysis of meteor data obtained at multiple stations will certainly provide valuable information on the mineralogical and morphological properties of cometary meteoroids.

We have demonstrated the validity of equation (5), which incorporates equation (3), but there is room for improvement of equation (5). Indeed, we cannot rule out the possibility that there is a better prescription for the relationship between the coordination number n_c and the volume filling factor ϕ of dust aggregates, compared with equation (3). For example, the classical model of Rumpf (1970) suggests

$$n_c = \frac{\pi}{1 - \phi}, \quad (6)$$

while Gundlach et al. (2018) considered that a reasonable prescription for the n_c – ϕ relationship of dust aggregates is given by van de Lagemaat et al. (2001):

$$n_c = \frac{c_1}{1 - \phi} - c_2, \quad (7)$$

with $c_1 = 3.08$ and $c_2 = 1.13$. Norman et al. (1971) proposed an extension of equation (3):

$$n_c = c_1 \exp(d_1 \phi) - c_2 \exp(d_2 \phi), \quad (8)$$

where $c_1 = 1.126$, $c_2 = 0.860$, $d_1 = 3.196$, and $d_2 = -3.50$. Figure 8 depicts these models for the n_c – ϕ relationships together with

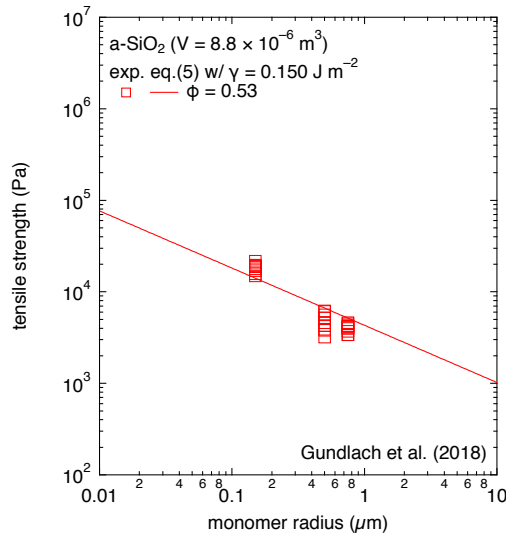


Figure 9. The dependence of tensile strength on the radius of monomers for dust aggregates expected from laboratory experiments and our formula. The open squares: experimental results by Gundlach et al. (2018).

the data for specific structures of granular matters. It turned out that equation (3) gives the highest n_c values in the range of $\phi \approx 0.4$ – 0.7 , compared with the other models.⁵ This could partly explain the reason that equation (5) tends to slightly overestimate the tensile strength of dust aggregates in the range of $\phi = 0.41$ – 0.66 measured by Blum & Schr apler (2004) and Blum et al. (2006). Therefore, we expect that a better choice of the n_c - ϕ relationship would improve a theoretical prediction for the tensile strength of porous dust aggregates.

There has been no consensus about the dependence of tensile strength σ on the radius r_0 of monomers among models for the tensile strength of dust aggregates: $\sigma \propto r_0^{-2.0}$ by Greenberg, Mizutani & Yamamoto (1995); $\sigma \propto r_0^{-5/3}$ by Wada et al. (2008); $\sigma \propto r_0^{-1.0}$ by Tatsuuma et al. (2019). It should be noted that these proportionalities are purely predictions by the respective models, but they have never been fully justified by experimental results up to date. Our model implies $\sigma \propto r_0^{-1.0}$ as a model of Tatsuuma et al. (2019), if the volume of dust aggregates is proportional to the third power of r_0 . However, as far as the same volume of dust aggregates is concerned, we predict that the tensile strength of porous dust aggregates shows a weaker dependence of monomer radius as $\sigma \propto r_0^{3/m-1}$ (crudely $\sigma \propto r_0^{-0.5 \pm 0.1}$ for $m = 5$ – 8). Currier & Schulson (1982) presented their experimental results of $\sigma \propto r_0^{-0.5}$ for aggregates of polycrystalline water ice grains with $\phi = 0.999$, although the volume filling factor of $\phi = 0.999$ would lie beyond the applicability of our model. Figure 9 depicts that the dependence of tensile strength on the radius of monomers measured for the same volume of dust aggregates by Gundlach et al. (2018) is consistent with equation (5). Our success in reproducing experimental and numerical results of tensile strength, irrespective of the composition and the size of monomers as well as the volume of the aggregates, presented in Sec 3 has given grounds for the proportionality of $\sigma \propto r_0^{3/m-1}$.

Skorov & Blum (2012) proposed that the tensile strength σ of dust aggregates increases with the volume of the aggregates, according to $\sigma \propto V^{2/15}$, up to millimeter sizes, and then decreases with the volume V of the aggregates, according to $\sigma \propto V^{-2/9}$. On the basis of numerical simulations, however, Seizinger et al. (2013) and Tatsuuma et al. (2019) concluded that the tensile strength of dust aggregates smaller than millimeter sizes does not depend on the volume of the aggregates⁶. Our formula given in equation (5) does not provide evidence for neither an increase in the tensile strength with the volume of small aggregates nor the volume independence of tensile strength. The top panels of Fig. 10 depicts the tensile strengths of dust aggregates numerically determined by Seizinger et al. (2013) at $\phi \approx 0.435$ (left) and by Tatsuuma et al. (2019) at $\phi = 0.1$ (right) as a function of the volume of their aggregates. Here, one may notice that numerical results of Seizinger et al. (2013) reveal a weak decline of tensile strength with the volume of their aggregates, while numerical results of Tatsuuma et al. (2019) are scattered around equation (5). By taking into account the fact that the numerical results of Seizinger et al. (2013) underestimated the tensile strength of dust aggregates by a factor of 2, their results are consistent with the volume effect of our formula given in equation (5). A lack of volume effects in the numerical results of Tatsuuma et al. (2019) could be attributed to the small size of porous ($\phi = 0.1$) dust aggregates between $N = 2^{10}$ – 2^{16} used in their simulations, because the size of the aggregates

⁵ Note that these models given in Eqs. (6)–(8) are not all, but merely three examples; There are plenty of formulae that provide a prescription for the relationship between the coordination number n_c and the volume filling factor ϕ (see van Antwerpen et al. 2010).

⁶ Seizinger et al. (2013) considered the volume effect in the range of $V = 4.8$ – 9.6×10^{-14} m³ ($40 \mu\text{m} \times 40 \mu\text{m} \times 30 \mu\text{m}$ – $40 \mu\text{m} \times 40 \mu\text{m} \times 60 \mu\text{m}$) and Tatsuuma et al. (2019) in the range of $V = 4.3 \times 10^{-17}$ – 2.7×10^{-15} m³ ($3.5 \mu\text{m} \times 3.5 \mu\text{m} \times 3.5 \mu\text{m}$ – $14 \mu\text{m} \times 14 \mu\text{m} \times 14 \mu\text{m}$).

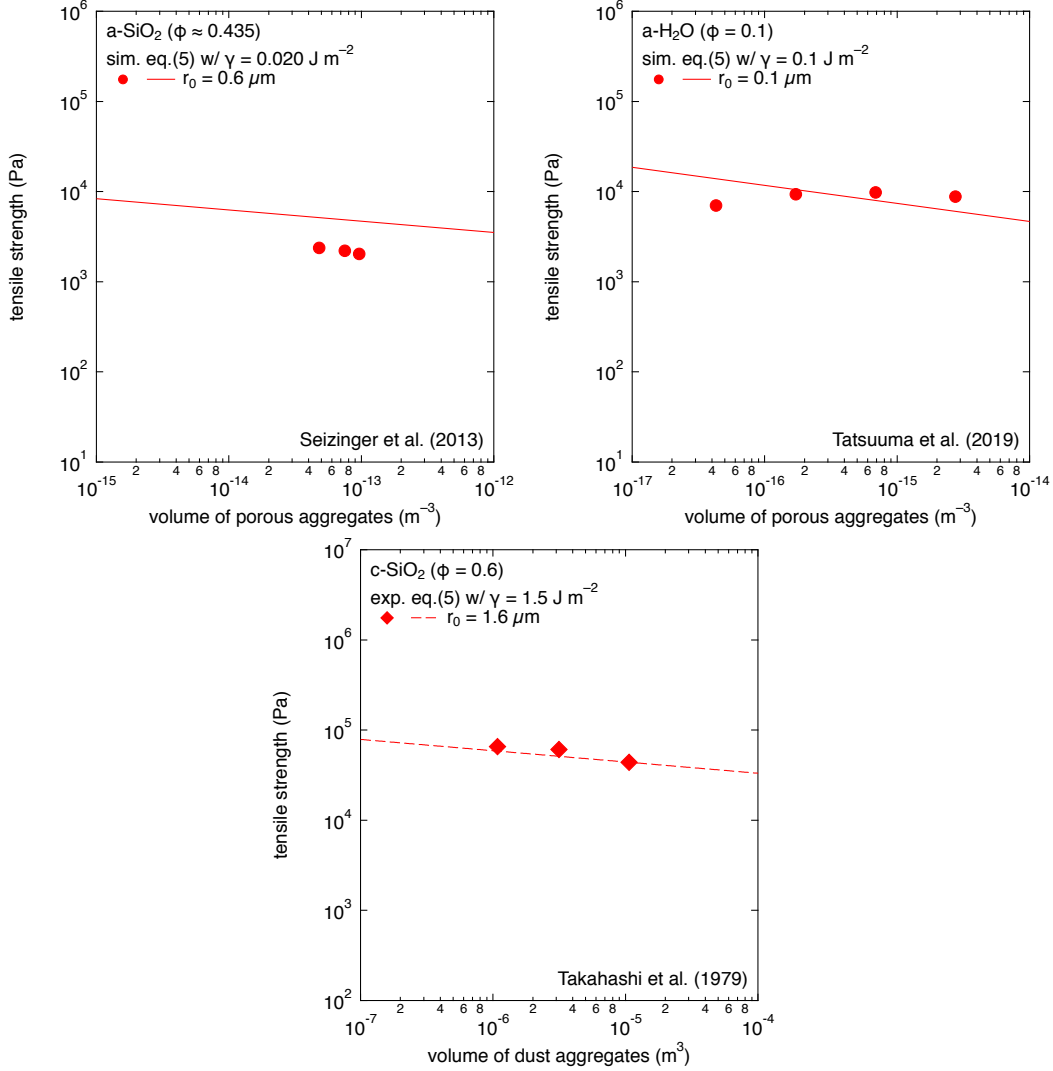


Figure 10. The volume effect of tensile strength for porous and compact dust aggregates expected from computer simulations, laboratory experiments, and our formula. Left top: numerical simulations by Seizinger et al. (2013); right top: numerical simulations by Tatsuuma et al. (2019); bottom: experimental results by Takahashi et al. (1979).

is on the same order as the maximum flaw size. Therefore, we anticipate that they would have also presented the volume effects, if larger volumes and higher volume filling factors were adopted in their simulations. Takahashi et al. (1979) have shown from their experiments that the tensile strength of silica powder beds with $\phi = 0.6$ gradually decreases with the volume of the powder beds, as expected by equation (5) (see the bottom panel of Fig. 10). Their results on the volume effect are again reproduced by equation (5) with $\gamma = 1.5 \text{ J m}^{-2}$, implying the establishment of siloxane bridges between monomers in the powder beds after intense compression. Since cometary dust and meteoroids also exhibit volume effects in the results of in-situ and ground-based observations (see Figs. 6 and 7), it is natural to consider that the tensile strength of dust aggregates gradually decreases with the volume of the aggregates, as expected from fracture mechanics (i.e. $\sigma \propto V^{-1/m}$).

As we have demonstrated throughout this paper using equation (5), the volume effects may play a vital role in the predicted values of tensile strength, unless the Weibull modulus is large enough. However, numerical results based on DEM simulations easily overlook this important effects as shown in the top panels of Fig. 10, due to a shortcoming of numerical simulations, which has a difficulty of dealing with a large span of volumes. As a result, from a theoretical point of view, there is a great demand for the determination of the Weibull modulus for astronomically relevant materials by laboratory experiments. Similarly important is a thorough inspection of a flaw size distribution in the laboratory, since the size distribution of flaws without a power law might violate the validity of equation (5). Therefore, we would like to encourage experimentalists to conduct their laboratory experiments with a wide size range of dust aggregates and to measure their tensile strengths and flaw-size distributions.

By taking into account uncertainties in the n_c - ϕ relationship, the Weibull modulus, and the volume filling factor of dust

aggregates consisting of swelling monomers in air, an analytical model of equation (5) for the tensile strength of dust aggregates is capable of reproducing results of laboratory experiments and computer simulations. In addition, we have revealed that the tensile strength of dust aggregates consisting of submicrometer-sized monomers with $r_0 \approx 0.1 \mu\text{m}$ in our model is consistent with observations of cometary dust and meteor showers. In summary, we succeed in restoring the consensus that porous dust aggregates, which were incorporated into comets in the solar nebula, consist of solar nebular condensates with radius $r_0 \approx 0.1 \mu\text{m}$.

ACKNOWLEDGEMENTS

We would like to thank Akiko M. Nakamura, Misako Tatsuuma, and Josep M. Trigo-Rodríguez for profitable discussion on the tensile strength of porous dust aggregates from experimental, numerical, and observational points of view, respectively, Irina L. San Sebastián and Jürgen Blum for sharing their experimental data with us prior to publication, and an anonymous reviewer for her/his comments that helped us to improve the manuscript. H.K. is grateful to JSPS's Grants-in-Aid for Scientific Research (KAKENHI #19H05085).

REFERENCES

- Arakawa S., Nakamoto T., 2016, *ApJ*, 832, L19
 Arakawa M., Nishino M., 1973, *Zairyo*, 22, 658
 Asakawa S., Jimbo G., 1967, *Zairyo*, 16, 358
 Atkinson B. K., 1984, *J. Geophys. Res.*, 89, 4077
 Atkinson B. K., Avdis V., 1980, *Int. J. Rock Mech. Min. Sci. Geomech. Abstr.*, 17, 383
 Axelson J. W., Piret E. L., 1950, *Ind. Eng. Chem.*, 42, 665
 Babadzhanyan P. B., Kokhirova G. I., 2008, *A&A*, 495, 353
 Ball A., Payne B. W., 1976, *J. Mater. Sci.*, 11, 731
 Beck J. M., Volpert V. A., 2003, *J. Colloid Interface Sci.*, 262, 162
 Bentley M. S., et al., 2016, *Nature* 537, 73
 Bérard V., Lesniewska E., Andrès C., Pertuy D., Laroche C., Pourcelot Y., 2002, *Int. J. Pharm.*, 247, 127
 Bika D. G., Gentzler M., Michaels J. N., 2001, *Powder Technol.*, 117, 98
 Blum J., Schräpler R., 2004, *Phys. Rev. Lett.*, 93, 115503
 Blum J., Schräpler R., Davidsson B. J. R., Trigo-Rodríguez J. M., 2006, *ApJ*, 652, 1768
 Borovička J., Spurný P., Koten P., 2007, *A&A*, 473, 661
 Borrero-López O., Hoffman M., Bendavid A., Martin P. J., 2010, *Thin Solid Films*, 518, 4911
 Brownlee D. E., 1985, *Annu. Rev. Earth Planet. Sci.*, 13, 147
 Brace W. F., Walsh J. B., 1962, *Amer. Miner.*, 47, 1111
 Carpin M., Bertelsen H., Bech J. K., Jeantet R., Risbo J., Schuck P., 2016, *Trends Food Sci. Technol.*, 53, 1
 Carpinteri A., 1994, *Int. J. Solids Struct.*, 31, 291
 Carpinteri A., Puzzi S., 2007, in Carpinteri A., Gambarova P. G., Ferro G., Plizzari G., eds, *Fracture Mechanics of Concrete and Concrete Structures*. Taylor & Francis. London, p. 31.
 Currier J. H., Schulson E. M., 1982, *Acta Mater.*, 30, 1511
 Danjo K., Iida K., Otsuka A., 1982, *J. Soc. Powder Technol. Japan*, 19, 530
 Darot M., Gueguen Y., Benchemam Z., Gaboriaud R., 1985, *Phys. Earth Planet. Inter.*, 40, 180
 Das S., Larson I., Young P., Stewart P., 2009, *Eur. J. Pharm. Sci.*, 38, 347
 Das S. C., Larson I., Morton D. A. V., Stewart P. J., 2010, *Langmuir*, 27, 521
 de Leeuw N. H., Manon F. M., Higgins A., Parker S. C., 1999, *J. Phys. Chem. B*, 103, 1270
 Fornasier S., et al., 2015, *A&A*, 583, A30
 Fujiwara Y., Ueda M., Sugimoto M., Sagayama T., Satake M., Furoue A., 2001, in Warmbein B., eds, *Proceedings of the Meteoroids 2001 Conference (ESA SP-495)*, ESTEC, Noordwijk. p. 123
 Goumans T. P. M., Wander A., Brown W. A., Catlow C. R. A., 2007, *Phys. Chem. Chem. Phys.*, 9, 2146
 Greenberg J. M., Mizutani H., Yamamoto, T., 1995, *A&A*, 295, L35
 Griffith A. A., 1921, *Phil. Trans. R. Soc. A*, 221, 163
 Groussin O., et al., 2015, *A&A*, 583, A32
 Gundlach B., et al., 2018, *MNRAS*, 479, 1273
 Hartley N. E. W., Wilshaw T. R., 1973, *J. Mater. Sci.*, 8, 265
 Hertz H., 1881, *J. Reine Angew. Math.*, 1882, 156
 Hohno H., Adachi S., 1982, *J. Dairy Sci.*, 65, 1421
 Hornung K., et al., 2016, *Planet. Space Sci.*, 133, 63
 Housen K. R., Holsapple K. A., 1999, *Icarus* 142, 21
 Jimbo G., Asakawa S., Soga N., 1968, *Zairyo*, 17, 540
 Johnson K. L., Kendall K., Roberts A. D., 1971, *Proc. R. Soc. Lond. Ser. A*, 324, 301
 Jones M. D., Young P., Traini D., 2012, *Adv. Drug Deliv. Rev.*, 64, 285
 Kamiya H., Kimura A., Yokoyama T., Naito M., Jimbo G., 2002, *Powder Technol.*, 127, 239
 Kendall K., 1987, in Briscoe B. J., Adams M. J., eds, *Tribology in Particulate Technology*, IOP Publishing, Bristol, p. 110

- Kendall K., Alford N. McN., Birchall J. D., 1987, *Proc. R. Soc. Lond. Ser. A*, 269
- Kendall K., Stainton C., 2001, *Powder Technol.*, 121, 223
- Kepler J., 1611, *Strena Seu De Nive Sexangula*. Tambach, Gottfried, Frankfurt a.M., p. 1
- Kimura H., Kolokolova L., Mann I., 2003, *A&A*, 407, L5
- Kimura H., Kolokolova L., Mann I., 2006, *A&A*, 449, 1243
- Kimura H., Wada K., Senshu H., Kobayashi H., 2015, *ApJ*, 812, 67
- Kimura H., Hilchenbach M., Merouane S., Paquette J., Stenzel O., 2020, *Planet. Space Sci.*, 181, 104825
- Klein C. A., 2009, *Opt. Eng.*, 48, 113401
- Kobayashi H., Kimura H., Yamamoto S., 2013, *A&A*, 550, A72
- Kolokolova L., Kimura H., Kiselev N., Rosenbush V., 2007, *A&A*, 463, 1189
- Kočova S., Pilpel N., 1972, *Powder Technol.*, 5, 329
- Kočova S., Pilpel N., 1973, *Powder Technol.*, 7, 51
- Lamy P. L., Grün E., Perrin J.-M., 1987, *A&A*, 187, 677
- Liu Q., Lu Z., Zhu M., Yuan Z., Yang Z., Hu Z., Li J., 2014, *Soft Matter*, 10, 6266
- Madiedo J. M., Trigo-Rodríguez J. M., Konovalova N., Williams I. P., Castro-Tirado A. J., Ortiz J. L., Cabrera-Canño J., 2013, *MNRAS*, 433, 571
- Mannel T., Bentley M. S., Schmied R., Jeszenszky H., Lévassieur-Regourd A. C., Romstedt J., Torkar K., 2016, *MNRAS*, 462, S304
- Maszara W. P., Goetz G., Caviglia A., McKittrick J. B., 1988, *J. Appl. Phys.*, 64, 4943
- Meisner T., Wurm G., Teiser J., 2012, *A&A*, 544, A138
- Meissner H. P., Michaels A. S., Kaiser R., 1964, *Ind. Eng. Chem. Proc. Des. Dev.*, 3, 202
- Murashov V. V., 2005, *J. Phys. Chem. B*, 109, 4144
- Murashov V. V., Demchuk E., 2005a, *J. Phys. Chem. B*, 109, 10835
- Murashov V. V., Demchuk E., 2005b, *Surf. Sci.*, 595, 6
- Naito M., Kato N., Jimbo G., Yokoyama T., 1986, *J. Soc. Powder Technol. Japan*, 23, 500
- Naito M., Usuda S., Kato N., Tsubaki J.-i., Jimbo G., 1987, *Powder Technol. Japan* 24, 455
- Nakamura A. M., Yamane F., Okamoto T., Takasawa S., 2015, *Planet. Space Sci.*, 107, 45
- Norman L. D., Maust E. E. Jr., Skolnick L. P., 1971, USBM, 658 United States. Government Printing Office, Washington D.C., USA
- Oda M., 1977, *Soils Found.*, 17, 29
- Okamoto H., Mukai T., Kozasa T., 1994, *Planet. Space Sci.*, 42, 643
- Okamoto T., Nakamura A. M., 2017, *Icarus*, 292, 234
- Pan D., Liu L.-M., Tribello G. A., Slater B., Michaelides A., Wang E., 2010, *J. Phys. Condens. Matter*, 22, 074209
- Parks G. A., 1984, *J. Geophys. Res.*, 89, 3997
- Patil S. P., Rege A., Sagardas, Itskov M., Markert B., 2017, *J. Phys. Chem. B*, 121, 5660
- Petrovic J. J., 2003, *J. Mater. Sci.*, 38, 1
- Pinson D., Zou R. P., Yu A. B., Zulli P., McCarthy M. J., 1998, *J. Phys. D*, 31, 457
- Rangsten P., Vallin Ö., Hermansson K., Bäcklund Y., 1999, *J. Electrochem. Soc.*, 146, 1104
- Reach W. T., Vaubailon J., Lisse C. M., Holloway M., Rho J., 2010, *Icarus*, 208, 276
- Rignanes G. M., De Vita A., Charlier J. C., Gonze X., Car R., 2000, *Phys. Rev. B*, 61, 13250
- Rumpf H. C. H., 1970, *Chem. Ing. Tech. (Weinh)*, 42, 538
- San Sebastián I. L., Dolf A., Blum J., Parisi M. G., Kothe S., 2020, *MNRAS*, submitted.
- Shchipalov Y. K., 2000, *Glass Ceram*, 57, 374
- Schwarz U. D., 2003, *J. Colloid Interface Sci.*, 261, 99
- Seizinger A., Speith R., Kley W., 2013, *A&A*, 559, A19
- Sindel U., Zimmermann I., 2001, *Powder Technol.*, 117, 247
- Skorov Y., Blum J., 2012, *Icarus*, 221, 1
- Smith W. O., Foote P. D., Busang P. F., 1929, *Phys. Rev.*, 34, 1271
- Sommerfeld R. A., 1974, *J. Geophys. Res.*, 79, 3353
- Steinpilz T., Teiser J., Wurm G., 2019, *ApJ*, 874, 60.
- Stengl R., Tan T., Gösele U., 1989, *Jpn. J. Appl. Phys.*, 28, 1735
- Steurer W., Apfalter A., Koch M., Ernst W. E., Holst B., Søndergård E., Parker S. C., 2008, *Phys. Rev. B*, 78, 035402
- Takahashi M., Katoh M., Suzuki S., Kobayashi T., 1979, *Zairyo*, 28, 819
- Takano K., Nishii K., Mukoyama A., Iwadate Y., Kamiya H., Horio M., 2002, *Powder Technol.*, 122, 212
- Tarasevich Y., 2006, *Theor. Experim. Chem.*, 42, 145
- Tatsuuma M., Kataoka A., Tanaka H., 2019, *ApJ*, 874, 159
- Traini D., Young P. M., Thielmann F., Acharya M., 2008, *Drug Dev. Ind. Pharm.*, 34, 992
- Trigo-Rodríguez J. M., Llorca J., 2006, *MNRAS*, 372, 655
- Tsubaki J., Jimbo G., 1984, *Powder Technol.*, 37, 219
- van Antwerpen W., du Toit C. G., Rousseau P. G., 2010, *Nucl. Eng. Des.*, 240, 1803
- van de Lagemaat J., Benkstein K. D., Frank A. J., 2001, *J. Phys. Chem. B*, 105, 12433
- Vigil G., Xu Z., Steinberg S., Israelachvili J., 1994, *J. Colloid Interface Sci.*, 165, 367
- Wada K., Tanaka H., Suyama T., Kimura H., Yamamoto T., 2008, *ApJ*, 677, 1296
- Wang X., Zhang Q., Li X., Ye J., Li L., 2018, *Minerals*, 8, 58
- Weidenschilling S. J., 1984, *Icarus*, 60, 553
- Weidenschilling S. J., 1997, *Icarus*, 127, 290
- Weidenschilling S. J., Donn B., Meakin P., 1989, in Weaver H. A., Danly L., Fall S., eds, *The Formation and Evolution of Planetary Systems*, Cambridge University Press, Cambridge. p. 131
- Woignier T., Phalippou J., 1988, *J. Non-Cryst. Solids*, 100, 404
- Yamamoto T., Hasegawa H., 1977, *Prog. Theor. Phys.*, 58, 816

- Yokoyama T., Fujii K., Yokoyama T., 1982, *Powder Technol.*, 32, 55
 York P., Pilpel N., 1972, *Mater. Sci. Eng.*, 9, 281
 Zhang J., Ebbens S., Chen X., Jin Z., Luk S., Madden C., Patel N., Roberts C. J., 2006, *Pharm. Res.*, 23, 401
 Zhuravlev L. T., 2000, *Colloids Surf. A*, 173, 1

APPENDIX A: INFLUENCE OF ADSORBED WATER MOLECULES ON THE VOLUME FILLING FACTOR

It is common practice that the volume filling factor ϕ of an agglomerate is determined by measuring the mass M of the agglomerate

$$\phi = \frac{M}{\rho V}, \quad (\text{A1})$$

where ρ is the density of constituent particles (i.e. $\rho \approx 2.0 \times 10^3 \text{ kg m}^{-3}$ for amorphous silica). The number N of particles in the agglomerate is given by

$$N = \frac{3V\phi}{4\pi r_0^3}. \quad (\text{A2})$$

If particles are hydrophilic and adsorb water molecules, then the radius of the particles increase from r_0 to r'_0 where $\Delta r_0 = r'_0 - r_0$ represents the thickness of water layers. The adsorption of water molecules reduces the mass of the agglomerate from M to M' :

$$M' = \frac{4}{3}\pi \left[r_0^3 \rho + (r_0'^3 - r_0^3) \rho_{\text{H}_2\text{O}} \right] N', \quad (\text{A3})$$

where $\rho_{\text{H}_2\text{O}}$ is the density of water (i.e. $\rho_{\text{H}_2\text{O}} = 1.0 \times 10^3 \text{ kg m}^{-3}$ and N' is the number of hydrophilic particles encased in the volume V with the filling factor ϕ :

$$N' = \frac{3V\phi}{4\pi r_0'^3}. \quad (\text{A4})$$

Accordingly, we have

$$\frac{M'}{\rho V} = \left\{ \left(\frac{r_0}{r'_0} \right)^3 \left[1 - \left(\frac{\rho_{\text{H}_2\text{O}}}{\rho} \right) \right] + \left(\frac{\rho_{\text{H}_2\text{O}}}{\rho} \right) \right\} \phi. \quad (\text{A5})$$

If the volume filling factor ϕ' of an agglomerate is determined by $\phi' = M'(\rho V)^{-1}$ in a laboratory experiment, then the value of the volume filling factor is underestimated, because $M'(\rho V)^{-1} < \phi$.

APPENDIX B: SURFACE ENERGY OF QUARTZ (CRYSTALLINE SILICA)

Axelsson & Piret (1950) listed theoretically evaluated values for the surface energy of quartz in the range of $\gamma = 0.51\text{--}2.3 \text{ J m}^{-2}$ and took a value of $\gamma = 0.98 \text{ J m}^{-2}$ to investigate their experimental results. Brace & Walsh (1962) determined the surface energy of quartz from their measurements by the crack-opening method in the range $\gamma = 0.41\text{--}1.03 \text{ J m}^{-2}$ depending on its crystallographic axes (see, also Tarasevich 2006). Using the same technique as Brace & Walsh (1962), Hartley & Wilshaw (1973) measured the surface energy of synthetic α -quartz to be $\gamma = 11.5 \pm 1.5 \text{ J m}^{-2}$ in air at room temperature. By using the Vickers hardness test, Atkinson & Avdis (1980) determined $\gamma = 0.46 \text{ J m}^{-2}$ for quartz (1010) and $\gamma = 1.34 \text{ J m}^{-2}$ for quartz (0001) in air at room temperature, while the surface energy for quartz (1010) was elevated to $\gamma = 1.77 \text{ J m}^{-2}$ at 200°C. Atkinson (1984) applied the crack-opening method to measure the surface energy of $\gamma = 3.49\text{--}4.83 \text{ J m}^{-2}$ for quartz in liquid water or moist air. Parks (1984) argued that the surface energy of quartz is as high as $\gamma = 2 \text{ J m}^{-2}$ in vacuum, by considering effects of adsorbed water molecules on the surface in laboratory experiments. Darot et al. (1985) applied the Vickers hardness test to estimate the surface energy of $\gamma = 10.75 \pm 0.15 \text{ J m}^{-2}$ for α -quartz (10 $\bar{1}$ 1) in argon at room temperature, while they observed a sudden drop of the surface energy down to $\gamma \sim 0.1 \text{ J m}^{-2}$ around the temperature of transition from α - to β -quartz (10 $\bar{1}$ 1), (10 $\bar{1}$ 0) and (0001). Ball & Payne (1976) estimated the surface energy of quartz to be $\gamma = 1.8\text{--}2.4 \text{ J m}^{-2}$ using an experimentally derived value of the Si-O bond energy. Rangsten et al. (1999) derived the surface energy of quartz to be $\gamma = 1.14\text{--}1.74 \text{ J m}^{-2}$ from their measurements of crack length at elevated temperatures using the crack opening technique. de Leeuw et al. (1999) and Steurer et al. (2008) computed the surface energy of α -quartz (0001) surface to be $\gamma = 1.92\text{--}2.77 \text{ J m}^{-2}$ and $\gamma = 1.48\text{--}4.0 \text{ J m}^{-2}$, respectively, using atomistic simulation techniques based on the Born model of ionic solids. Rignanesi et al. (2000) have determined the surface energy for the (0001) surface of α -quartz by performing molecular dynamics simulations to be $\gamma = 0.80\text{--}4.0 \text{ J m}^{-2}$ depending on the model of the surface geometry. The surface energy for quartz calculated by the periodic density functional theory (DFT) ranges from $\gamma = 2.6$ to 3.2 J m^{-2} by Murashov & Demchuk (2005a,b), from $\gamma = 1.1$ to

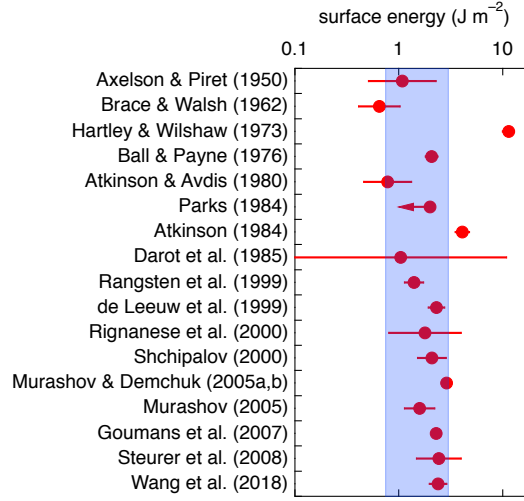


Figure B1. The surface energies γ of quartz estimated by different methods and authors (the filled circles). Shaded area: $\gamma = 1.5 \text{ J m}^{-2}$ within a factor of 2.

2.2 J m^{-2} by [Murashov \(2005\)](#), and from $\gamma = 2.2$ to 2.4 J m^{-2} by [Goumans et al. \(2007\)](#). Theoretical calculations by [Shchipalov \(2000\)](#) suggest $\gamma = 2.875 \text{ J m}^{-2}$ for α -cristobalite on the plane $\{001\}$, $\gamma = 1.511 \text{ J m}^{-2}$ for α -cristobalite on the plane $\{111\}$, $\gamma = 1.567 \text{ J m}^{-2}$ for β -cristobalite, and $\gamma = 1.707 \text{ J m}^{-2}$ for β -quartz. DFT calculations by [Wang et al. \(2018\)](#) gave results that the O-middle termination of quartz (001) surfaces has the lowest surface energy of $\gamma = 1.969 \text{ J m}^{-2}$ and the surface energies of the O-rich termination and the Si termination are $\gamma = 2.892 \text{ J m}^{-2}$ and $\gamma = 2.896 \text{ J m}^{-2}$, respectively. Figure B1 compiles the surface energies γ of quartz estimated by different methods and authors, while most of the values are confined to $\gamma = 1.5 \text{ J m}^{-2}$ within a factor of 2.

This paper has been typeset from a $\text{\TeX}/\text{\LaTeX}$ file prepared by the author.